

Opportunistic Third-Party Backhaul for Cellular Wireless Networks

Russell Ford, *Student Member, IEEE*, Changkyu Kim, *Student Member, IEEE*, Sundeep Rangan, *Senior Member, IEEE*

Abstract—With high capacity air interfaces and large numbers of small cells, *backhaul* – the wired connectivity to base stations – is increasingly becoming the cost driver in cellular wireless networks. One reason for the high cost of backhaul is that capacity is often purchased on leased lines with guaranteed rates provisioned to peak loads. In this paper, we present an alternate *opportunistic backhaul* model where third parties provide base stations and backhaul connections and lease out excess capacity in their networks to the cellular provider when available, presumably at significantly lower costs than guaranteed connections. We describe a scalable architecture for such deployments using open access *femtocells*, which are small plug-and-play base stations that operate in the carrier’s spectrum but can connect directly into the third party provider’s wired network. Within the proposed architecture, we present a general user association optimization algorithm that enables the cellular provider to dynamically determine which mobiles should be assigned to the third-party femtocells based on the traffic demands, interference and channel conditions and third-party access pricing. Although the optimization is non-convex, the algorithm uses a computationally efficient method for finding approximate solutions via dual decomposition. Simulations of the deployment model based on actual base station locations are presented that show that large capacity gains are achievable if adoption of third-party, open access femtocells can reach even a small fraction of the current market penetration of WiFi access points.

Index Terms—cellular networks, 3GPP LTE, femtocells, access pricing, utility maximization.

I. INTRODUCTION

Cellular wireless networks have been traditionally designed on the premise that the wireless interface is the bottleneck for system throughput and capacity. However, a surprising recent trend is that *backhaul*, meaning the wired connectivity to the base stations, is increasingly becoming the dominant cost driver in many networks [1], [2]. Even for comparatively lower data rate pre-4G systems, backhaul already accounted for a significant percentage of the operating costs (30 to 50% by some estimates [3], [4]). Higher data rate 4G systems combined with the increasing adoption of a large numbers of small cell deployments [3] will require even greater costs in the backhaul, particularly in markets where the operator does not have universal fiber access.

This work presents a novel deployment model for cellular providers that would enable the rising costs of backhaul networks to be mitigated by offloading traffic to third-party

backhaul connections. The basic premise is that backhaul services are currently purchased with guaranteed service level agreements (SLAs) along dedicated lines [5], which come at a significant cost for operators. These SLAs must generally be provisioned for the *peak* data rates. However, due to variations in loading and channel conditions, much of the purchased capacity goes to waste.

We propose that, rather than provisioning these links for the peak demand, cellular networks should be able to dynamically leverage excess capacity on existing backhaul links provided by third-party entities. The role of this third party may be played by other services providers (i.e. wireline ISPs) or even broadband customers, the very end-users themselves.

The third parties can provide connectivity to the operator’s subscribers through *femtocells* [6]–[8], which are small, low-cost, cellular base stations that operate in the provider’s spectrum but are connected into the third party’s backhaul. The network can then offload mobile subscribers to the third party femtocells and the cellular provider would reimburse the third party for use of the backhaul resources (and possibly cover the one-time cost of the femtocell as well). The key is to offload traffic *opportunistically* when third parties have excess backhaul capacity. Since this capacity would only be purchased when used and since mobile traffic would generally represent only a small increment in average demand at most enterprises and residences, the opportunistic capacity can presumably be purchased at much a lower cost than guaranteed lines to base stations.

In addition, significant progress has been made in making femtocells completely self-organizing with “plug-and-play” installation [9], [10], implying that third-party femtocells would have minimal operating costs. In this way, opportunistic backhaul with third-party open-access femtocells can provide a scalable model for high-density, high-capacity deployments at low cost.

We describe a potential architecture for third-party opportunistic backhaul model within the LTE/SAE framework [11] (see Section II). Within this architecture, we consider one of the key technical problems, namely the optimization of *user association*: The cellular provider’s network must dynamically assign mobile subscribers between the operator-controlled base stations and third party femtocells based on channel and interference conditions, backhaul capacity, traffic demands and third party access pricing. We present a general optimization formulation for this problem using a recently-developed methodology in [12], which itself was based on [13]. The user association optimization problem is generally non-convex,

This material is based upon work supported by the National Science Foundation under Grant No. 1116589.

R. Ford (email: rford02@students.poly.edu) and S. Rangan (email: srangan@poly.edu) are with the Polytechnic Institute of New York University, Brooklyn, NY.

but following [12], we show that the optimization admits a dual decomposition that enables application of efficient approximate augmented Lagrangian methods. The methodology is extremely general and enables joint optimization for load balancing and interference coordination and can incorporate a large class of interference models, network topologies and pricing schemes.

To evaluate the potential capacity increase for this opportunistic backhaul model, we present a simple simulation where we assume open access femtocells can be co-located at a small fraction (between 2 and 25%) of the locations where current residential and enterprise WiFi access points are deployed. Basing our simulations on reported location data of WiFi access points and cellular base stations and industry standard cellular evaluation models [14], we show that large capacity gains are possible with offload into third-party networks and we discuss the potential costs of investment in the third-party model compared to the additional operator-deployed or leased line infrastructure required to support an equivalent gain in system throughput.

A. Related work

Although femtocells have been traditionally used for improving coverage in private residences and enterprises [6]–[8], open access femtocells deployed explicitly for wide-area coverage have also been considered – see, for example, Qualcomm’s *neighborhood small cells* whitepaper [15]. That work showed significant capacity gains would be possible with open-access LTE femtocells placed at a small fraction (10%) of residences. The analysis, however, does not explicitly consider the issues of backhaul usage and third-party charging, which are the main focus of this paper.

A comparable business model is also found in public WiFi networks such as FON, which boasts itself as the “world’s largest WiFi network” [16]. FON members, called “Foneros”, agree to allow other Foneros to securely connect to their custom home WiFi AP and, in return, gain access the millions of other hotspots hosted by members of the community. Under one of the available membership plans, users are incentivized to provide reliable WiFi service by being compensated per-byte of data traffic consumed by other Foneros. The FON business model has been tremendously successful in recent years, bringing in 28 million Euro in revenue during 2010 [17]. In this work, we consider offload to cellular, rather than WiFi, which has the advantage of better support for mobility and interference management. Moreover, in the model presented, the network makes all cell selection decisions and is responsible for paying third parties for offloaded traffic; third-party vs. provider ownership is transparent to the mobile subscribers who see all base stations as belonging to a single network.

A mathematical evaluation of pricing schemes for mobile subscribers is presented in [18], which concludes that operators can maximize revenue by offering femto services to all customers at a flat rate, that is, not as an extra value-added service but part of the basic package. We adopt this method of subscriber charging in our model, which we believe has the added benefit of encouraging femtocell adoption. The utility

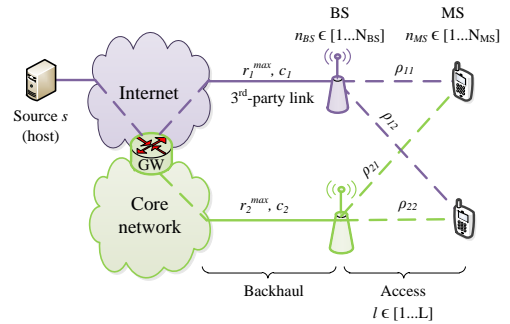


Fig. 1: Heterogeneous network architecture where operator-controlled cells (drawn in green) are combined with third-party controlled femtocells (drawn in purple).

for data consumers is often modeled by a logarithmic function of rate (a special case of iso-elastic utility), which has the rational basis of expressing the decreasing marginal payoff of rate experienced by users [19]–[21].

Understanding the shape of the supply-side utility curve for third-party backhaul providers is not as straightforward, however. Intuitively, a monopolist operator wants to offer a price for backhaul capacity that maximizes their net utility, which is a function of the average or total throughput seen by users as well as the cost of connectivity over third-party links. Although we consider the operator to be a price taker under this model, if the third-party provider is an individual end-user with leased broadband capacity, we assume their supply-side price elasticity is likely to be very inelastic since they will accept any price offered for their excess bandwidth (seeing as how they would otherwise get nothing) [21]. This dynamic becomes significantly more complex, requiring a game-theoretic approach to analysis, when we consider a competitive market where one or more broadband ISPs offer resources to one or more mobile service providers and the price of said resources may be a time-varying function of demand.¹

In this paper, we forgo an analysis of competitive markets in favor of investigating the relationship between a single cellular provider (with existing macrocellular infrastructure) and many 3rd-party backhaul providers. We assume this baseline model in order to demonstrate a general framework for determining net utility gains and couch an upper bound on the incentive that could be offered while still increasing operator revenue.

II. SYSTEM ARCHITECTURE

As described in the Introduction, we propose that third parties use open-access femtocells to provide service to the mobile subscribers of a cellular operator. The basic network architecture is shown in Fig. 1 which follows the standard model of 3GPP LTE/SAE heterogeneous networks [9], [11]. As shown, there are two classes of base station cells in the proposed model: *operator-controlled* and *third-party*. The operator-controlled cells (set BS_M) are the standard BS nodes

¹Such multi-sided markets are the subject of [22], which introduces a bidding system through which providers compete for network resources.

connected directly to the operator core network and managed by the operator. These are typically macro- or microcells, hence the subscript M . The third party cells (set BS_F), are the open access femtocell BS nodes installed by a third party and connected to the third-party ISP network, i.e. the Internet.

In the proposed model, the third-party and operator first agree on some access pricing, perhaps a cost per unit time or unit data that the operator will reimburse the third-party provider when mobile subscribers connect to their network – we will see that our optimization methodology can incorporate a range of pricing models. Then, at any time, the network can choose to assign mobiles to either operator-controlled or third-party cells depending on the channel and interference conditions, traffic loading and access pricing.

There are several convenient features of this deployment model:

- *Deployment ease and scalability:* Most importantly, the use of third party femtocells offers a scalable and cost effective approach to increase capacity: Since femtocells are low-cost, plug-and-play devices, third parties can install these devices themselves, thereby immediately creating an abundance of cell sites virtually for free. In addition, as described in the Neighborhood Small Cell concept [15], when the cellular operator also provides a broadband residential and enterprise ISP service (such as Verizon’s FiOS or AT&T’s U-Verse service), they could include a femtocell within the WiFi access point given to the subscriber, thereby automatically enabling femtocell capabilities in every subscriber’s location.
- *Direct operator to third party economic relationship:* The economic interaction with respect to access pricing can be made entirely between the cellular operator and the third-party provider – the mobile subscriber need not be involved. This arrangement is possible since, in networks such as 3GPP LTE, for mobiles in connected mode, the network makes all decisions on which cells serve the mobiles [11]. Thus, the network and third-party provider can come to an agreement on access pricing, and then the network can decide, in each time instant, whether to have its mobiles served by the third party cells based on channel conditions, network load, and other factors.
- *Transparency to mobiles:* Related to the above point is that, from the mobile station perspective, both classes of base station cells – third-party and operator-controlled – are completely identical, potentially using the same radio access technology and potentially operating in the same spectrum band.² Thus, the third party vs. operator ownership is transparent to the mobiles. This feature is beneficial since the mobile user is really concerned with the quality of the connectivity and has no interest *per se* in who provides that connection.
- *Correctly matched incentives:* Since the operator will only reimburse third parties when Open Subscriber Group (OSG) mobiles are served by the third party cell, the operator does not need to enforce proper installment

and operation of the femtocell. Third parties will be naturally incentivized to keep their femtocell on and well-positioned to attract the operator to move its mobile subscribers onto its network to receive payment. On the other hand, if the third-party network is busy and cannot support the additional mobile traffic, the third-party is free to shut off or cap the rate to the femtocell and the cellular operator can adjust its cell selection decisions accordingly. As we will see in the next section, our user association algorithm can account for backhaul limits on the third party cells.

- *Minimal changes to existing standards:* All the hooks necessary for the proposed third-party offload can be handled within the existing cellular standards. For example, in 3GPP LTE, the mobiles already provide the network with all the measurement reports necessary to determine the airlink conditions and received signal strengths to make the handover decisions. Also, in the current LTE network model, all traffic from the public Internet is routed first through a gateway³ before being tunneled to the base stations, whether the base stations cells are operator-controlled or operated by a third-party outside the operator core network [11].⁴ Thus, the network can both monitor the exact amount of time and data to each cell type for charging and to measure link quality.

III. USER ASSOCIATION OPTIMIZATION

As mentioned above, a key technical challenge in realizing the proposed architecture is that the cellular provider requires a good algorithm for *user association*: the cellular provider must determine, in each time instant, how to assign mobile users between the third-party and operator-controlled cells while accounting for channel and interference conditions, access prices and loading. To this end, we use a utility maximizing algorithm proposed in [12] and [13] for optimized user association in heterogeneous networks, incorporating access price into the utility function.

A. Optimization Formulation

Returning to Fig. 1, let MSi , $i = 1, \dots, N_{MS}$ denote the set of mobile stations and BSj , $j = 1, \dots, N_{BS}$ set of base station cells, the latter set including both operator-controlled and third-party cells. For each MSi , let $\Gamma_{MS}(i)$ denote the indices j such that BSj can potentially serve the mobile. Similarly, let $\Gamma_{BS}(j)$ be the set of mobiles potentially served by BSj . Also, let r_{ij} and w_{ij} be the rate and bandwidth allocated to MSi from BSj for $j \in \Gamma_{MS}(i)$. Let \bar{r}_i^{MS} and \bar{r}_j^{BS} be the total rate to the MSi and BSj respectively, which must satisfy the constraints

$$\bar{r}_i^{MS} \leq \sum_{j \in \Gamma_{MS}(i)} r_{ij}, \quad \bar{r}_j^{BS} \geq \sum_{i \in \Gamma_{BS}(j)} r_{ij}. \quad (1)$$

³The gateway, in this case, serves the combined function of the LTE P-GW/S-GW. We consider these to be co-located nodes.

⁴Note that while protocols such as Selected IP Traffic Offload (SIPTO) [23] allow small cell traffic to bypass the CN and be offloaded directly to the Internet, we do not consider this case here since network and transport layer mobility functions need to be handled by the CN in any case.

²Our interference model presented in the following section addresses co-channel and separate channel deployments.

Absent of carrier aggregation [24], mobiles in LTE are typically only served by one cell at a time. If we let \mathbf{r} be the vector of the rates r_{ij} , we will denote this single path constraint as

$$\mathbf{r} \in \mathbf{S} := \{\mathbf{r} : r_{ij} = 0 \text{ for all but one } j \in \Gamma_{\text{MS}}(i)\}. \quad (2)$$

Now, following [12], we attempt to find rates to maximize some utility function of the form

$$U(\bar{\mathbf{r}}^{MS}) = \sum_{i=1}^{N_{MS}} U_i(\bar{r}_i^{MS}), \quad (3)$$

for some utility functions $U_i(\bar{r}_i^{MS})$. To account for the backhaul costs that the operator must pay the third party providers, we assume there is a cost of the form

$$C(\bar{\mathbf{r}}^{BS}) = \sum_{j=1}^{N_{BS}} C_j(\bar{r}_j^{BS}), \quad (4)$$

where $C_j(\bar{r}_j^{BS})$ is the cost for the traffic on BS j that the operator will have to pay the third-party that owns BS j . BS nodes belonging to BS_M represent operator-deployed cells connected over statically-provisioned backhaul links will generally have zero cost ($C_j(\bar{r}_j^{BS}) = 0$), since we consider existing infrastructure to be a sunk cost for the operator. Nodes in BS_F are third-party cells and have some positive cost ($C_j(\bar{r}_j^{BS}) > 0$) that they charge the operator. The cost functions $C_j(\bar{r}_j^{BS})$ can also be used to incorporate rate limits on either the third-party or operator-deployed cells due to finite backhaul capacity on those cell sites.

The goal is to maximize a *net utility*, $U(\bar{\mathbf{r}}^{MS}) - C(\bar{\mathbf{r}}^{BS})$, subject to constraints on the rates. The rate limits depend on the channel and interference conditions, which we model using a linear mixing interference model proposed in [25]. Let z_{ij} be the interference power on the link from BS j to MS i . As described in [12], assuming that the base stations radiate a fixed power per unit bandwidth, the vector of interference powers must satisfy a constraint of the form

$$\mathbf{z} \geq \mathbf{G}\mathbf{w}, \quad (5)$$

where \mathbf{w} is the vector of bandwidth allocations and \mathbf{G} is an appropriate gain matrix. The rate on the links must then satisfy

$$r_{ij} \leq w_{ij} \rho_{ij}(z_{ij}), \quad (6)$$

where $\rho_{ij}(z_{ij})$ is the spectral efficiency (rate per unit bandwidth) as a function of the interference level z_{ij} . Also, the bandwidths must satisfy some constraints of the form

$$\sum_{i \in \Gamma_{\text{BS}}(j)} w_{ij} \leq \bar{w}_j, \quad (7)$$

where \bar{w}_j is the total bandwidth available in BS j . By appropriate selection of the gain matrix \mathbf{G} , this formulation can incorporate both co-channel deployments of the third-party and operator-controlled cells where the two types of cells use the same bandwidth and interfere with one another, or separate channel deployments where there is no interference.

Now let $\boldsymbol{\theta}$ be the vector of all the unknowns

$$\boldsymbol{\theta} = (\mathbf{r}, \bar{\mathbf{r}}^{BS}, \bar{\mathbf{r}}^{MS}, \mathbf{w}, \mathbf{z})^T. \quad (8)$$

The constraints (1), (5) and (7) can be replaced by inequality constraints represented in a matrix form

$$\mathbf{A}\boldsymbol{\theta} \leq \mathbf{b}, \quad (9)$$

for appropriate choice of the matrix \mathbf{A} and vector \mathbf{b} . We can then write the user association problem as the optimization

$$\max_{\boldsymbol{\theta}} U(\bar{\mathbf{r}}^{MS}) - C(\bar{\mathbf{r}}^{BS}) \quad (10a)$$

$$s.t. \quad \mathbf{A}\boldsymbol{\theta} \leq \mathbf{b} \quad (10b)$$

$$\mathbf{r} \leq \mathbf{w} \cdot \rho(\mathbf{z}) \quad (10c)$$

$$\mathbf{r} \in \mathbf{S}, \quad (10d)$$

where the constraint (10c) is a vector shorthand for the constraints (6).

B. Dual Decomposition Algorithm

The optimization (10) is, in general, non-convex due to the nonlinearity of the interference rate-interference constraints (10c) and the single path constraints (2). However, following [12], we can find an approximate solution to this problem in two steps. First, we initially ignore the single path constraint (2). The resulting optimization will produce a vector with rates on all paths to the mobiles. We then simply “truncate” the solution to take the path with the largest rate. This truncation procedure is well-known in networking theory [26] and often introduces little error, since the multipath solution tends to concentrate on dominant single paths.

Unfortunately, even with the multipath approximation, the optimization (10) will be non-convex. However, as in [12], we can show that the optimization admits a separable dual decomposition. Specifically, the Lagrangian corresponding to the optimization (10) without the single path constraint (10d) is given by

$$L(\boldsymbol{\theta}, \boldsymbol{\mu}) := U(\bar{\mathbf{r}}^{MS}) - C(\bar{\mathbf{r}}^{BS}) - \boldsymbol{\mu}^T g(\boldsymbol{\theta}), \quad (11)$$

where $g(\boldsymbol{\theta})$ is the vector of constraints

$$g(\boldsymbol{\theta}) = \left(\mathbf{A}\boldsymbol{\theta} - \mathbf{b}, \mathbf{r} - \mathbf{w} \cdot \rho(\mathbf{z}) \right)^T, \quad (12)$$

and $\boldsymbol{\mu} \geq 0$ is the vector of dual parameters partitioned conformably with $g(\boldsymbol{\theta})$

$$\boldsymbol{\mu} = (\boldsymbol{\mu}^\theta, \boldsymbol{\mu}^r)^T. \quad (13)$$

Now central to using dual optimization methods is the ability to compute the maxima of the form

$$\hat{\boldsymbol{\theta}}(\boldsymbol{\mu}) := \arg \max_{\boldsymbol{\theta}} L(\boldsymbol{\theta}, \boldsymbol{\mu}) - \Phi(\boldsymbol{\theta}), \quad (14)$$

for some augmenting function $\Phi(\boldsymbol{\theta})$. Using a similar argument as in [12], the following lemma shows that, under the assumption of a separable augmenting function $\Phi(\cdot)$, the optimization (14) admits a separable dual decomposition.

Lemma 1: Let $\Phi(\boldsymbol{\theta})$ be any separable function of the form

$$\begin{aligned} \Phi(\boldsymbol{\theta}) &= \Phi(\mathbf{r}, \bar{\mathbf{r}}^{BS}, \bar{\mathbf{r}}^{MS}, \mathbf{w}, \mathbf{z}) \\ &= \sum_{ij} \left[\phi_{ij}^r(r_{ij}) + \phi_{ij}^z(w_{ij}, z_{ij}) \right] \\ &\quad + \sum_j \phi_j^{BS}(\bar{r}_j^{BS}) + \sum_i \phi_i^{MS}(\bar{r}_i^{MS}) \end{aligned} \quad (15)$$

for some functions $\phi_{ij}^r(\cdot)$, $\phi_j^{BS}(\cdot)$, $\phi_i^{MS}(\cdot)$ and $\phi_{ij}^z(\cdot)$. Let $\boldsymbol{\mu}$ be any vector of Lagrange parameters and let $\hat{\boldsymbol{\theta}}(\boldsymbol{\mu})$ be the corresponding maxima for the dual optimization augmented by $\Phi(\boldsymbol{\theta})$, namely

$$\begin{aligned} \hat{\boldsymbol{\theta}}(\boldsymbol{\mu}) &= (\hat{\mathbf{r}}, \hat{\mathbf{r}}^{BS}, \hat{\mathbf{r}}^{MS}, \hat{\mathbf{w}}, \hat{\mathbf{z}}) \\ &:= \arg \max_{\boldsymbol{\theta}} [L(\boldsymbol{\theta}, \boldsymbol{\mu}) - \Phi(\boldsymbol{\theta})]. \end{aligned} \quad (16)$$

Then, the components of $\hat{\boldsymbol{\theta}}(\boldsymbol{\mu})$ are given by the solutions to the optimizations

$$\begin{aligned} \hat{r}_{ij} &\in \arg \min_{r_{ij}} [\phi_{ij}^r(r_{ij}) + (\lambda_{ij}^r + \mu_{ij}^r)r_{ij}] \\ \hat{r}_j^{BS} &\in \arg \min_{\bar{r}_j^{BS}} [C_j(\bar{r}_j^{BS}) + \phi_j^{BS}(\bar{r}_j^{BS}) + \lambda_j^{BS}\bar{r}_j^{BS}] \\ \hat{r}_i^{MS} &\in \arg \max_{\bar{r}_i^{MS}} [U_i(\bar{r}_i^{MS}) - \phi_i^{MS}(\bar{r}_i^{MS}) - \lambda_i^{MS}\bar{r}_i^{MS}] \end{aligned}$$

and

$$\begin{aligned} (\hat{w}_{ij}, \hat{z}_{ij}) &\in \arg \max_{w_{ij}, z_{ij}} [\mu_{ij}^r w_{ij} \rho_{ij}(z_{ij}) \\ &\quad - \lambda_{ij}^z z_{ij} - \lambda_{ij}^w w_{ij} - \phi_{ij}^z(w_{ij}, z_{ij})], \end{aligned}$$

where the dual parameters $\boldsymbol{\mu}$ are partitioned as in (13) and the parameters λ are the components

$$\boldsymbol{\lambda} = (\boldsymbol{\lambda}^r, \boldsymbol{\lambda}^{BS}, \boldsymbol{\lambda}^{MS}, \boldsymbol{\lambda}^w, \boldsymbol{\lambda}^z) := \mathbf{A}^T \boldsymbol{\mu}^\theta,$$

where the vector $\boldsymbol{\lambda}$ has been partitioned conformably with $\boldsymbol{\theta}$ in (8).

Proof: This result follows immediately from the separable structure of the objective function and constraints. ■

The lemma shows that the vector optimization (16) separates into a set of simple one and two-dimensional optimizations over the components of $\boldsymbol{\theta}$ and can thus be computed easily for any dual parameters $\boldsymbol{\lambda}$. As discussed in [12], this separability property has two key consequences that follow immediately from standard optimization theory [27]: First, one can use weak duality to efficiently to compute an upper bound on the maximum net utility. Specifically, the net utility is bounded by

$$\max_{\boldsymbol{\theta}} U(\boldsymbol{\theta}) - C(\boldsymbol{\theta}) \leq \max_{\boldsymbol{\mu}} L(\boldsymbol{\theta}, \boldsymbol{\mu}), \quad (18)$$

for any dual parameters $\boldsymbol{\mu} \geq 0$. Moreover, the right-hand side of (18) is convex in $\boldsymbol{\mu}$, and since the dual maxima is separable, one can compute its value and gradient for any $\boldsymbol{\mu}$. Thus, one can efficiently minimize the right hand side of (18), providing a computable upper bound on the net utility. Although the dual upper bound may not be tight (i.e. the optimization may not be strongly dual), the bound provides a computable metric under which any approximate algorithm can be compared against.

A second consequence of a computable dual maxima is that one can efficiently implement several well-known augmented Lagrangian techniques to find approximate maxima to the net utility $U(\boldsymbol{\theta}) - C(\boldsymbol{\theta})$. These methods include various inexact versions of alternating direction method of multiplier methods [28], [29] – see [12] for more details.

A valuable property is that this dual decomposition applies in very general circumstances. In particular, one can consider

arbitrary cost and utility functions, and SNR-to-rate mappings $\rho_{ij}(\cdot)$. Thus, the framework provides a tractable and general methodology for a large class of networks, interference scenarios and pricing schemes with computable upper bounds on performance.

IV. SYSTEM EVALUATION

A. Evaluation Methodology

To evaluate the opportunistic backhaul model, we conducted a network simulation using a simplified version of industry-standard models for evaluating multi-tier networks [14], [30], [31]. Our goal was to determine the gain in network capacity as a function of the number of third party providers and offloaded backhaul capacity.

Two deployment models were considered: *real-world* and *stochastic*. In the real-world model, the operator-controlled BS locations were based on actual cell sites as reported in the OpenCellId database, which has logged data for over 500,000 individual cells in the US [32]. For the third-party femtocells, following [15], we assume that the third party femtocells can be co-located with current residential and enterprise WiFi access points (APs) – the theory being that the owners of these WiFi APs would be the potential third parties to offer connectivity to the mobile subscribers. The WiFi AP locations were estimated from the freely-available Wigle.net database. Contributors to the Wigle project have compiled over 88 million unique observations of WiFi stations across the globe [33].

Our simulations considered two test locations: a 1km² area of the East Village in Manhattan, New York City – representative of a dense urban deployment – and a similar-sized area in Passaic, NJ as representative of a typical suburban deployment. Fig. 2 is an aerial map of WiFi APs and cell sites in the selected area of Manhattan as reported in the OpenCellId and Wigle.net databases, plotted together in Google EarthTM [34]. For the observed population of WiFi APs in the 1km² areas of NYC and Passaic, NJ, we uniformly sample a percentage of these nodes in the domain {2%, 5%, 10%, 15%, 20%}, which represents the adoption rate of third-party WiFi owners that agree to provide backhaul service to the cellular operator through a femtocell co-located at a WiFi AP.

The equivalent number of nodes for both the urban and suburban locations is given in Table I. We immediately see that, according to the databases we sampled, there are more than 2000 WiFi APs for each cellular microcell in Manhattan. This vast number of WiFi APs suggests that if, even a small fraction of open-access femtocells can be co-located at current WiFi locations, the cellular capacity can be massively increased.

For completeness, we compare our results based on real-world locations with industry-standard *stochastic models* [14], [31] used widely in evaluating cellular systems. For the urban scenario in both the real-world and stochastic models, we take the operator-deployed nodes to be microcells, which are omnidirectional transmitters with power, bandwidth and other parameters coinciding with the 3GPP urban microcell model in [14], [31]. Femtocells are similarly configured based on these



Fig. 2: Google EarthTM map of reported microcell locations (blue balloons) and a fraction of the WiFi sites (green circles) in the East Village, Manhattan. Since the WiFi access points vastly outnumber the current cellular base stations (more than 2000 to 1 in this case), cellular capacity can be significantly increased if femtocells can be co-located at even a small fraction of the WiFi sites.

TABLE I: Number of operator-controlled and third-party cells and number of UEs in the urban and suburban test cases

Environment	Node Type	Number of Nodes
Urban micro-only and micro+femto	Micro	$N_M = 17$
	Femto	$N_F \in \{722, 1805, 3610, 5415, 7220\}^*$
	UE	$N_{MS} = 425$ (25/micro)
Suburban: macro-only and macro+femto	Macro	$N_M = 9$
	Femto	$N_F \in \{66, 165, 330, 495, 660, 825\}^*$
	UE	$N_{MS} = 225$ (25/macro)

* N_F computed from the adoption rate: {2%, 5%, 10%, 15%, 20%} of observed WiFi APs

parameters and are subject to a maximum backhaul rate in the set {10, 20, 30, 40, 50} Mbps.⁵ These values for the rate constraint parameter are assigned uniformly over the set of femtocells. For the suburban scenario (for both real-world and stochastic models), we consider operator BSs to be three-way-sectorized macrocells. For the stochastic models, the densities of the operator-controlled macro/microcells and third-party femtocells were adjusted to match the densities observed in the real-world data. Other salient parameters are given in Table II. Note that the femtocells have an additional 20 dB of path loss to account for the wall loss assuming the femtocell is deployed indoors.

For each of the scenarios (urban / suburban and real-world / stochastic), we follow the standard evaluation methodology in [14], [31] to assess the downlink capacity. Specifically, we generate 10 random instances of each of the networks; each instance is called a *drop*. In each random drop, we run the optimization described in Section III to determine the

optimal user association between the third-party and operator-controlled cells. In reality, we envision that this optimization would be conducted in the operator's network.

In conducting the optimization, we assume a similar model as [35], where the spectral efficiency $\rho_{ij}(z_{ij})$ in (6) is given by the Shannon capacity with a loss of 3 dB with a maximum value of 4.8 bps/Hz (corresponding to 64-QAM at rate 5/6). For the utility (3), we assume a proportional fair metric $U_i(\bar{r}_i^{MS}) = \log(\bar{r}_i^{MS})$. The backhaul capacity is assumed to be zero for operator-controlled cells, while third-party cells charge a linear cost so that

$$C_j(\bar{r}_j^{BS}) = \begin{cases} p\bar{r}_j^{BS}, & j \in BS_F \text{ (i.e. femtocell)} \\ 0, & j \in BS_M \text{ (i.e. macro/microcell)} \end{cases} \quad (19)$$

where p represents the cost per unit backhaul capacity in the femtocell relative to the utility. The price p will be varied.

TABLE II: Network model parameters

	Parameter	Value
Urban microcell	Topology	Uniform with wrap-around
	Total TX power	30 dBm
	BW	10 MHz (FDD DL)
	Antenna pattern	omni
	Micro \leftrightarrow UE path loss	$15.3 + 37.6 \log_{10}(R)$ (R in km)
	Micro \leftrightarrow UE log-normal shadowing	10dB std. dev; 50% inter-site correlation; 100% intra-site correlation
Femtocell	Topology	Uniform with wrap-around
	Total TX power	20 dBm
	BW	10 MHz (FDD DL)
	Antenna pattern	omni
	Femto \leftrightarrow UE path loss	$15.3 + 37.6 \log_{10}(R) + 20dB$ (R in km)
	Femto \leftrightarrow UE log-normal shadowing	8dB std. dev
	Backhaul max rate	$r_{max} \in \{10, 20, 30, 40, 50\}$ Mbps uniformly assigned to nodes
Suburban macrocell	Topology	Hexagonal (3-way sectorized) with wrap-around
	Total TX power	46 dBm
	BW	10 MHz (FDD DL)
	Antenna pattern	$A(\theta) = -\min\{12(\frac{\theta}{\theta_{3dB}})^2, A_m\}$
	Macro \leftrightarrow UE path loss	$15.3 + 37.6 \log_{10}(R)$ (R in km)
	Macro \leftrightarrow UE log-normal shadowing	8dB std. dev
Global	Carrier frequency	2.1 GHz
	Total area	1000x1000m
	UE distribution	Uniform, 25 per macro/microcell
	Mobility	constant
	Traffic model	full buffer
	Fading	none
	Link capacity	$C = W * \min(\log(1 + 10^{-\frac{\beta}{10}} SNR), \rho_{max})$ $\beta = 3dB$ (loss from Shannon cap.*) ρ_{max} (max. spectral efficiency)

*We determine the achievable rate based on the loss from Shannon capacity, as discussed in [35].

⁵Backhaul rate constraint values are based on broadband services commonly offered by many ISPs in the US.

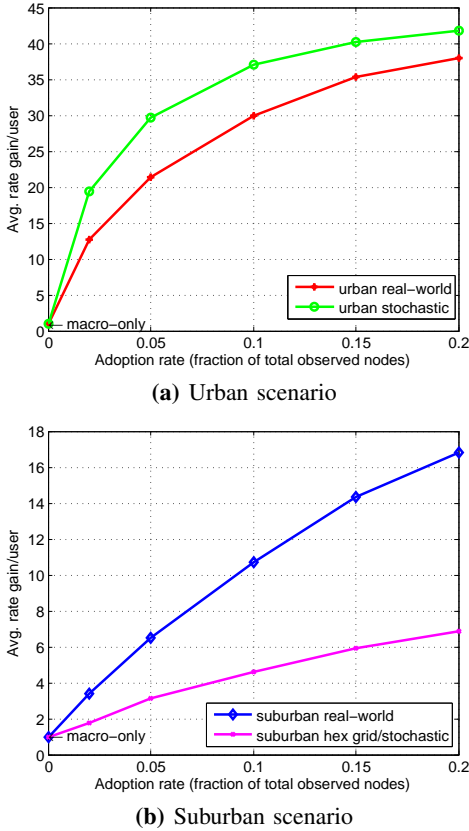


Fig. 3: Average rate gain as a function of the adoption rate in urban and suburban deployments. We see that if even a small fraction (5%) of WiFi owners agree to install open-access femtocells, cellular capacity can increase more than 20 fold in a dense urban environment and a factor of 6 in a suburban deployment.

B. Potential Capacity Gain with Offloading

To estimate the maximum possible capacity gain with third-party offload, we first consider the case where the third-party providers lease their capacity at zero cost (i.e. $p = 0$ in (19)). Fig. 3 shows that the gain in mean throughput per mobile as a function of the adoption rate – the fraction of WiFi AP locations where open-access femtocells are co-located. We see that the total capacity can be increased significantly. For example, a 5% adoption yields more than 20x increase in user throughput in the real-world urban setting and a 6x increase in the real-world suburban model. The maximum gain in the suburban model is not as high as the urban setting since the density of third-party cells is lower. Also, the maximum gains in both cases begin to saturate since we fix the number of UEs per macros. Therefore, adding more femtocells eventually has little value – a phenomena also observed in [15]. The finite backhaul rates on the femtocells also limits the gain.

Fig. 4 similarly plots the increase in the cell-edge throughput. As defined in [14], the cell-edge rate is the rate of the 5% percentile UE in each drop. We see similar gains at the cell edge as the mean gains, suggesting that the gains are uniformly experienced across the cell. Table III states the gain value for the urban case at the 5% adoption.

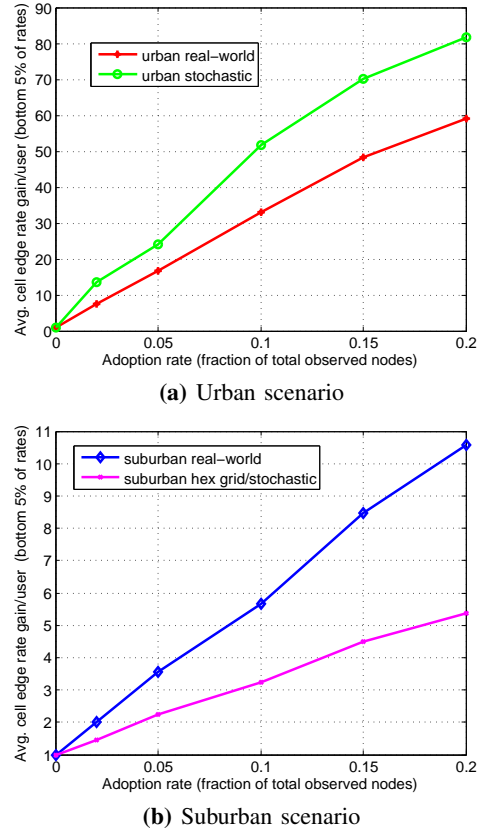


Fig. 4: Average 5% cell-edge rate gain as a function of the adoption rate in urban and suburban deployments.

TABLE III: Capacity and cell edge gains with 5% femtocell adoption based on the urban real-world model.

Scenario	Macro-only	Macro+Femto	Gain
Avg. UE rate (Mbps)	0.63	13.38	21.39
Avg. 5% cell edge rate (Mbps)	0.08	1.36	16.71
Utility (geometric mean rate, Mbps)	0.41	9.35	22.66

C. Adding Third-Party Pricing

The results in the previous subsection assumed that the relative cost of the third-party backhaul (the variable p in (19)) was zero. Of course, in reality, third parties will not generally offer backhaul for free, so we need to consider the capacity gain with non-zero pricing. Unfortunately, there is no way to directly determine the “correct” relative price p to use in the evaluation without some economic analysis relating the potential revenue increase to the operator from increased capacity (as measured by the utility) versus the cost to the operator of the third-party backhaul. However, such analysis is beyond the scope of this study, although business models have been considered elsewhere, e.g. [36].

What is relevant for this work is to show that our net utility

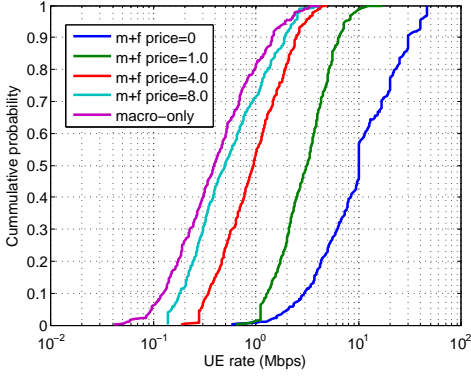


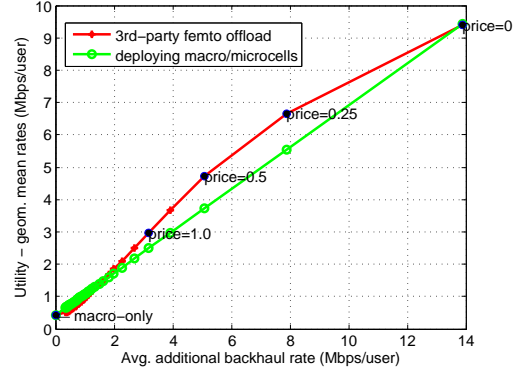
Fig. 5: Distribution of the UE rates for micro+femto urban real-world model with femto price $p \in \{0, 1, 4, 8\}$ and 5% adoption. Also, plotted is the macro-only distribution which corresponds to the price $p = \infty$.

maximization optimization can incorporate pricing, whatever the correct pricing is. As an illustration, we fix the adoption rate at 5% and run the micro+femto optimization for different prices p in (19).⁶ Fig. 5 plots the resulting rate distributions across the UEs for the different prices. As we would expect, as the price is increased, the number of users scheduled on third-party links along with the volume of offloaded traffic decreases as a result of the algorithm’s penalization of such users. The optimal allocation of resources therefore tends to involve these links less and less. As $p \rightarrow \infty$, the rate distribution approaches the distribution using only the operator-controlled microcells.

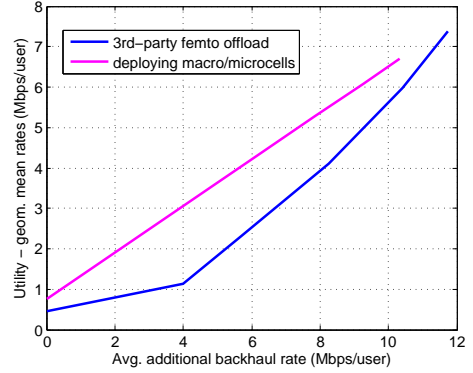
Also, although we cannot assess the absolute economic value of femtocell offload, we can conduct the following simple comparison: Suppose the operator wishes to increase capacity of its network. We compare the following two methods:

- *Increase operator-controlled cells:* In this method, the operator does not use any femtocells and increases capacity by adding operator-controlled micro/macrocells only, i.e. traditional *cell splitting*. To simulate this scenario, we imagine a network with all the parameters being the same, except that the density of the micro/macrocells is increased by some factor $\alpha \geq 1$. Increasing the density in this manner will incur a variety of costs to the operator including the capital and operating expenses of the new base stations as well as the cost of the additional backhaul. For the moment, we will only consider the additional backhaul costs. Then, as we vary α , we can estimate the gain in network capacity as a function of the additional backhaul.
- *Femto offload:* As an alternate approach, we imagine that the operator adds no new micro/macro base station cells of its own and relies entirely on purchasing capacity via femto offload. To simulate this scenario, we fix an adoption rate at some reasonable value (we assume 5%), and then increase network capacity by lowering the relative cost p in (19), from $p = \infty$ (where the operator

⁶It should be noted that loading price p is unitless (as far as the resource assignment algorithm is concerned) and simply represents the weight of the penalty incurred on net utility.



(a) Urban scenario



(b) Suburban scenario

Fig. 6: Average utility as a function of additional backhaul, comparing adding operator-controlled micro/macrocells only vs. relying entirely on femtocell offload. For the femtocell offload case, we assume a 5% adoption rate and vary the amount of backhaul used on the femtocells.

uses no femtocell offload) to $p = 0$ (where the network purchases any capacity on femtocells without regard to cost). Then, we can again measure the increase in network capacity as a function of the additional backhaul costs, where the additional backhaul in this case is on the third-party femtocells.

The results of this comparison are shown in Fig. 6. Plotted is the system utility as a function of the additional backhaul required for both methods – adding operator-controlled macro/microcells, or offloading to femtocells on existing backhaul. We measure capacity via the utility. Since we assume a proportional fair utility, $\sum_i \log(\bar{r}_i^{MS})$, the utility is equivalent to the geometric mean rate $(\prod_i \bar{r}_i^{MS})^{1/N_{MS}}$. The geometric mean rate is a better measure of network capacity than average rate since it penalizes mobiles with lower rates more significantly. Nevertheless, although it is not plotted, very similar curves would be observed with either arithmetic mean rate or cell edge throughput.

We see from Fig. 6 that, for the urban scenario, increasing the utility requires roughly the same amount of additional backhaul whether deploying more operator-controlled cells or using femtocell offload. In the suburban scenario, the femtocell offload requires significantly more additional backhaul for small increases in utility, but requires only modestly more additional backhaul for larger increases in capacity.

Now, as discussed in the Introduction, it is likely that the backhaul from femtocell offload would be significantly lower cost than the purchasing leased lines with guaranteed rates needed for operator-controlled macro/microcells. Moreover, adding operator-deployed cells incurs additional costs including site acquisition, infrastructure expenses and network maintenance [36]. Nevertheless, quantifying the exact savings would require further economic analysis.

CONCLUSIONS

We have presented a model for operators to offset backhaul costs by leveraging existing capacity from third-parties. In the proposed model, third parties install open-access femtocells in their networks and the cellular operator can then opt to move subscribers onto third party cells for a fee. The problem of dynamically assigning users between the third-party and operator-controlled cells is formulated as an optimization problem. A dual decomposition algorithm is presented that is extremely general and can incorporate channel and interference conditions, traffic demands, backhaul capacity and access pricing. To evaluate the model, we considered deployments where the third party femtocells were co-located with existing WiFi APs. Due to the large numbers of WiFi APs relative to base station cell sites, our simulations suggest that network capacity be significantly increased even if only a small fraction (say 5%) of current WiFi owners deploy open-access femtocells. The gains are particularly large in dense urban areas where our data suggests there are some 2000 WiFi APs per operator cell. Our optimization can also incorporate a variety of pricing mechanisms by the third parties, but determining the correct price will need analysis beyond the scope of this study. However, our simulations show that, whatever is the correct price, the additional backhaul to increase capacity is similar for both adding more operator-controlled cells or offloading to third-party femtocells. Thus, assuming third party backhaul can be offered at a lower rate than leased lines for operator-controlled cells, the savings of the proposed method can be significant. In this way, opportunistic backhaul can offer a scalable, low-cost method to increase network capacity and address the growing demands on cellular wireless networks.

REFERENCES

- [1] D. Webster, "Solving the mobile backhaul bottleneck," http://blogs.cisco.com/sp/solving_the_mobile_backhaul_bottleneck, Apr. 2009.
- [2] C. Mathias, "Fixing the cellular network: Backhaul is the key," <http://www.networkworld.com/community/print/35920>, Dec. 2008.
- [3] H. Claussen, L. T. W. Ho, and L. Samuel, "Financial analysis of a pico-cellular home network deployment," Jun. 2007, pp. 5604–5609.
- [4] Senza Fili Consulting, "Crucial economics for mobile data backhaul," Whitepaper available at <http://cfnl.com/sites/all/files/userfiles/files/CB-002070-DC-LATEST.pdf>, 2011.
- [5] S. Chia, M. Gasparroni, and P. Brick, "The next challenge for cellular networks: backhaul," *IEEE Microwave Magazine*, vol. 10, no. 5, pp. 54–66, May 2009.
- [6] V. Chandrasekhar, J. G. Andrews, and A. Gatherer, "Femtocell networks: A survey," *IEEE Comm. Mag.*, vol. 46, no. 9, pp. 59–67, Sep. 2009.
- [7] D. López-Pérez, A. Valcarce, G. de la Roche, and J. Zhang, "OFDMA femtocells: A roadmap on interference avoidance," *IEEE Comm. Mag.*, vol. 47, no. 9, pp. 41–48, Sep. 2009.
- [8] J. G. Andrews, H. Claussen, M. Dohler, S. Rangan, and M. C. Reed, "Femtocells: Past, present, and future," *IEEE J. Sel. Areas Comm.*, vol. 30, no. 3, Apr. 2012.
- [9] J. Zhang and G. de la Roche, *Femtocells: Technologies and Deployment*. Chichester, UK: John Wiley & Sons, 2010.
- [10] J. Ramiro and K. Hamied, Eds., *Self-Organizing Networks (SON): Self-Planning, Self-Optimization and Self-Healing for GSM, UMTS and LTE*. Wiley, 2011.
- [11] M. Olsson, S. Sultana, S. Rommer, L. Frid, and C. Mulligan, *SAE and the Evolved Packet Core: Driving the Mobile Broadband Revolution*. Academic Press, 2009.
- [12] C. Kim, R. Ford, Y. Qi, and S. Rangan, "Joint interference and user association optimization in cellular wireless networks," arXiv preprint, Apr. 2013.
- [13] Q. Ye, B. Rong, Y. Chen, M. Al-Shalash, C. Caramanis, and J. G. Andrews, "User association for load balancing in heterogeneous cellular networks," *IEEE Trans. Wireless Comm.*, Dec. 2013.
- [14] 3GPP, "Further advancements for E-UTRA physical layer aspects," TR 36.814 (release 9), 2010.
- [15] Qualcomm, "Neighborhood small cells for hyperdense deployments: Taking hetnets to the next level," [online] <http://www.qualcomm.com/media/documents/files/qualcomm-research-neighborhood-small-cell-deployment-model.pdf>, Feb. 2013.
- [16] Fon, <http://corp.fon.com/>.
- [17] R. Wauters, "Fon ended 2010 with 3.35 million wifi hotspots, 28 million in revenues," <http://techcrunch.com/2011/02/01/fon-ended-2010-with-3-35-million-wifi-hotspots-e28-million-in-revenues-2/>, Feb. 2011.
- [18] S.-Y. Yun and Y. Yi, "The economic effects of sharing femtocells," *IEEE J. Sel. Areas Comm.*, vol. 30, no. 3, pp. 595–606, Apr. 2012.
- [19] F. P. Kelly, A. K. Maulloo, and D. K. H. Tan, "Rate control for communication networks: shadow prices, proportional fairness and stability," *Journal of the Operational Research Society*, vol. 49, no. 3, pp. 237–252, Mar. 1998.
- [20] L. A. DaSilva, "Pricing for qos-enabled networks: A survey," *IEEE Communications Surveys & Tutorials*, vol. 3, no. 2, pp. 2–8, 2000.
- [21] M. Yuksel and S. Kalyanaraman, "Elasticity considerations for optimal pricing of networks," Jul. 2003, pp. 163–168.
- [22] L. T. W. Ho, F. Mullany, H. Claussen, and L. Samuel, "Autonomous organization of wireless network transport in a multi-provider environment," Apr. 2005, pp. 719–724.
- [23] 3GPP, "Local IP Access and Selected IP Traffic Offload," TR 23.829 (release 10), 2010.
- [24] G. Yuan, X. Zhang, W. Wang, and Y. Yang, "Carrier aggregation for LTE-Advanced mobile communication systems," *IEEE Comm. Mag.*, vol. 48, no. 2, pp. 88–93, 2010.
- [25] S. Rangan and R. Madan, "Belief propagation methods for intercell interference coordination in femtocell networks," *IEEE J. Sel. Areas Comm.*, vol. 30, no. 3, pp. 631–640, Apr. 2012.
- [26] M. Pióro and D. Medhi, *Routing, Flow and Capacity Design in Communication and Computer Networks*. Elsevier, 2004.
- [27] J. Nocedal and S. J. Wright, *Numerical Optimization*. Springer Verlag, 2006.
- [28] S. Boyd, N. Parikh, E. Chu, B. Peleato, and J. Eckstein, "Distributed optimization and statistical learning via the alternating direction method of multipliers," *Found. Trends Mach. Learn.*, vol. 3, no. 1, 2010.
- [29] X. Zhang, M. Burger, and S. Osher, "A unified primal-dual algorithm framework based on Bregman iteration," *SIAM J. Sci. Comput.*, vol. 46, pp. 20–46, 2011.
- [30] Femto Forum, "Interference management in OFDMA femtocells," Whitepaper available at www.femtoforum.org, Mar. 2010.
- [31] ITU, "M.2134: Requirements related to technical performance for IMT-Advanced radio interfaces," Technical Report, 2009.
- [32] OpenCellId, <http://www.opencellid.org/>.
- [33] Wigle, "Wigle frequently asked questions," <https://wigle.net/gps/gps/main/faq/>.
- [34] Google, "Google earth (version 7)," <http://www.google.com/earth>, 2013.
- [35] P. Mogensen, W. Na, I. Z. Kovács, F. Frederiksen, A. Pokhariyal, K. I. Pedersen, T. Kolding, K. Hugl, and M. Kuusela, "LTE capacity compared to the Shannon bound," in *Proc. IEEE VTC*, 2007.
- [36] Signals Research Group, "Femtocell Business Case," Femto Forum Whitepaper, Apr. 2009.